INTERNATIONAL INSTITUTE OF WELDING
A world of joining experience

Delegation of Austria

IIW Document XIII-2416-12

Contribution to the fatigue enhancement of thin-walled, high-strength steel joints by high frequency mechanical impact treatment

M. Leitner, M. Stoschka and W. Eichlseder

Montanuniversität Leoben, Chair of Mechanical Engineering, Austria

Abstract

It is well known that the fatigue strength of welded structures is in general independent from the material strength. Nevertheless, in case of high-strength steels it is possible to increase the fatigue behaviour by post treatment processes significantly.

This paper deals with the effect of high frequency mechanical impact (HFMI) for mild construction steel (*S355*) up to ultra high-strength steel (*S960*) on fatigue. The experiments imply fatigue tests on butt welds, T-joints and longitudinal attachments on five millimetres, thin-walled specimens. All specimens were produced by a semi-automatic, single-layer weld process which leads to a very high manufacturing quality without interior defects like gas pores or lack of fusion. The main lot was additionally HFMI treated at the weld toe to improve the fatigue level further on.

Extensive fatigue tests at a tumescent stress ratio of $R=0.1$ were done until burst fracture. In case of the longitudinal stiffeners, the amount of technical crack initiation was additionally determined by strain gauge measurement and subsequent evaluation.

The fatigue assessment was performed in accordance to the nominal and the notch stress approach, taking the HFMI condition into account. In case of the nominal stress approach, a benign thinness factor was applied. The applicability of a strength magnification adjustment, considering yield strength for HFMI treated joints, is depicted in case of the nominal stress assessment. Finally, a novel method is outlined to assess the notch stress fatigue behaviour of HFMI treated joints made of high-strength steel.

The evaluated fatigue results are only valid for five millimetres, thin-walled joints postulating a high manufacturing quality. Further work focuses on the validation of the introduced HFMI-fatigue enhanced notch stress model, especially for increased wall thicknesses and higher stress ratios.

Keywords

High frequency mechanical impact (HFMI), Fatigue strength improvement, Fatigue assessment, Notch stress approach, High-strength steel.

1 Introduction

In the finite lifetime area, the fatigue behaviour of welded high-strength steel joints is beneficial due to the increased yield limit. In regard to the high-cycle fatigue zone, the notch topography, the microstructure in the heat-affected-zone (HAZ), and the residual stress state influence the fatigue lifetime in a major way. According to the conservative recommendation [1], the fatigue life is independent of the yield strength of welded steel components. To assess the local fatigue strength of welded and HFMI post treated high-strength steel joints, fatigue tests using three different thin-walled (t_{eff}=*5 mm*) welded specimen types are investigated. Figure 1 illustrates the studied specimen types, ranging from butt joint, root surface in grinded condition, over T-joint to longitudinal attachment.

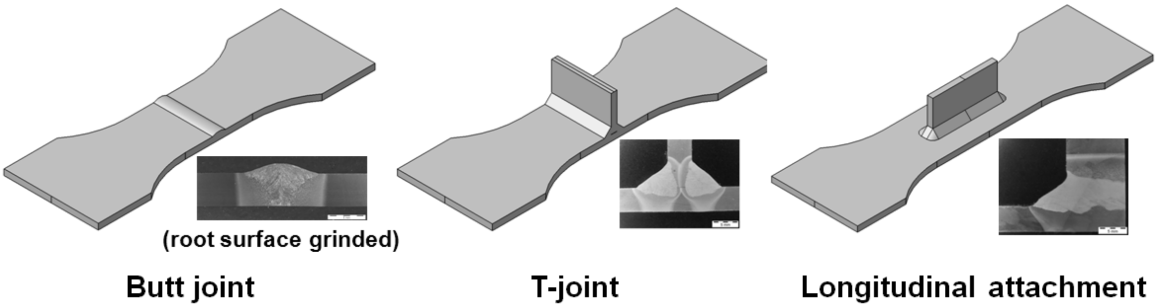

Figure 1: Investigated weld specimen types

Two low-alloyed high-strength steels *S690* and *S960,* and for comparative purposes a common construction steel *S355,* with a sheet thickness of *5 mm* are used as different base materials. All plates were sand blasted before welding. For the as welded condition, the structural detail dependent nominal stress range is defined in [1] as FAT, characteristic fatigue strength at two million cycles considering a probability of survival of *97.7 %*. Figure 2 depicts the nominal stress FAT-classes of the three examined joints.

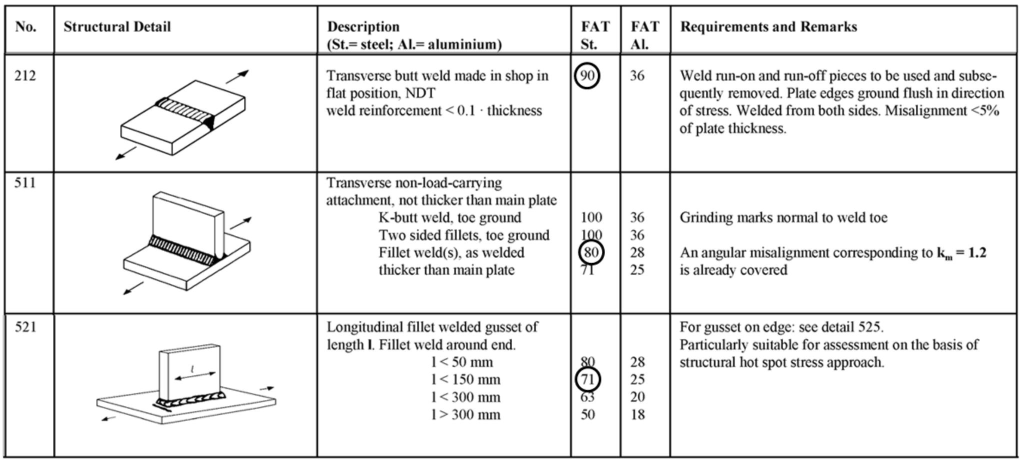

No.	Structural Detail	Description (St.= steel; Al.= aluminium)	FAT St.	FAT Al.	Requirements and Remarks
212		Transverse butt weld made in shop in flat position, NDT weld reinforcement < 0.1 · thickness	90	36	Weld run-on and run-off pieces to be used and subsequently removed. Plate edges ground flush in direction of stress. Welded from both sides. Misalignment <5% of plate thickness.
511		Transverse non-load-carrying attachment, not thicker than main plate			
		K-butt weld, toe ground	100	36	Grinding marks normal to weld toe
		Two sided fillets, toe ground	100	36	
		Fillet weld(s), as welded	80	28	An angular misalignment corresponding to k_m = 1.2 is already covered
		thicker than main plate	71	25	
521		Longitudinal fillet welded gusset of length l. Fillet weld around end.			For gusset on edge: see detail 525. Particularly suitable for assessment on the basis of structural hot spot stress approach.
		l < 50 mm	80	28	
		l < 150 mm	71	25	
		l < 300 mm	63	20	
		l > 300 mm	50	18	

Figure 2: Recommended nominal stress FAT-values for the investigated steel joints [1]

In the nominal stress concept, the fatigue strength enhancement for higher strength steel welds (f_y > *355 MPa*) improved by hammer or needle peening is expressed by a bonus factor of *1.5* [1]. This factor is applied to the recommended stress range. An overview of the existing post weld treatment methods, their application and the recommended benefit in fatigue is given in [2]. Recent research results [3, 4, 5] observed that the fatigue strength of improved HFMI treated welds increases with material yield strength. In [3], an extensive study including *228* experimental test data points showed that the fatigue benefit can be expressed by an increase of *12.5 %* for every *200 MPa* material strength growth ,choosing $f_{y,0}$ = *355 MPa* as base material strength reference.

2 Objectives

In this contribution, an evaluation of the fatigue behaviour of HFMI treated joints using the nominal and the notch stress concept for the different investigated joints is given. The goal is to assess methodical the benefit of the HFMI treatment for thin-walled high-strength steels. The examined work packages are:

- Experimental fatigue tests to gain the influence of the base material yield strength and the stress concentration factor at the weld toe on the fatigue behaviour of welded (without post treatment) and HMFI treated steel joints.
- Application of the existing recommendation to consider HFMI in the nominal stress concept and verification of the experimental data to published results.
- Proposal of a S/N-model to consider the HFMI treatment in the notch stress approach.

3 Experimental Investigations

Preliminary investigations [6,7], concerning the fatigue testing of welded joints, showed that a ratio of ten to one between width and thickness of the base plate ensures a plain strain state at the centre and encourages technical crack initiation in this homogenous region. In the course of the welding process, an optimal weld seam performance with high quality welds and reproducible results is obtained to minimize the influence of weld quality on the fatigue behaviour [8]. After welding and cool down to room temperature; half of each specimen lot is additionally post treated by HFMI. The post treatment is shown in Figure 3 for the three investigated joints.

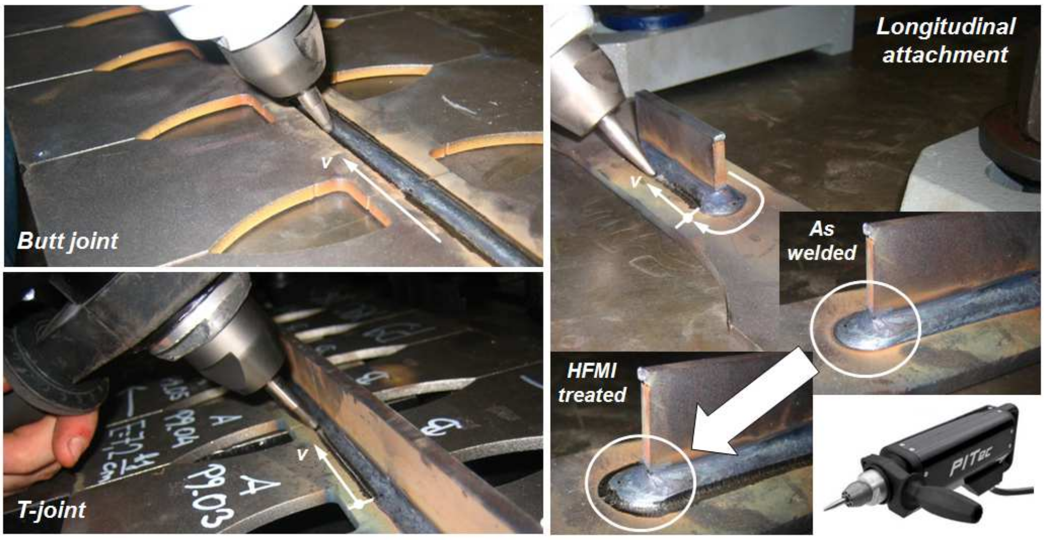

Figure 3: High frequency mechanical impact treatment (HFMI)

The high frequency mechanical impact treatment is done using the PIT (Pitec) [9] device. For the pneumatic actuation energy, a common industrial air pressure of *6 bar* (*0.6 MPa*) is needed. Comparative tests showed that a sufficient post treatment quality can be obtained when a treatment velocity of *v=20 to 30 cm/min* and a frequency of *90 Hz* is operated. The radius of the hardened pin used in this study is *R=2 mm,* which fits to the weld seam size of the investigated specimens [10]. The post treatment is applied on the welded specimens without additional static pre-stressing or former cyclic damage. Due to the HFMI treatment, the pulsed transaction of the hardened pin rounds out the curvature of the weld toe region and thereby reduces the geometric stress concentration factor at the weld toe. In addition, compressive stresses are induced which counteract the superposition of residual weld and external load applied tensile stresses. [11]
In total, over *three-hundred* specimens were tested with a constant tumescent testing load using a stress ratio of *R=0.1*. The abort criterion for the fatigue tests is total rupture and the run-out level is set to a number of fifty million load cycles.

3.1 Influence of Wall Thickness

In the IIW-recommendation [1], additional fatigue strength modifications, such as the effective mean stress factor *f(R)* and the thickness factor *f(t),* are defined. The effective mean stress factor *f(R)* is applicable both to the nominal and the notch stress concept, whereas the thickness factor *f(t)* is only valid for use in the nominal stress approach and not in local methods. Residual stress measurements of the investigated specimens [12] outlined a residual stress state above $0.2 \cdot f_y$ at the weld toe region. Therefore, no beneficial consideration of the effective mean stress factor *f(R)* is applicable. In case of the nominal stress approach, the fatigue strength is defined for a reference plate thickness of $t_{ref}=25\ mm$. For thicknesses greater than this value a reduction of the fatigue strength by the factor *f(t)*, see Equation 1, is recommended [1]. In the same way a benign thinness effect might be considered, but it has to be verified by experimental tests.

$$f(t) = \left(\frac{t_{ref}}{t_{eff}}\right)^n \tag{1}$$

For the numerical assessment of the benign thinness effect, a calculation of the notch stress concentration factors K_t at the weld toe for the three investigated specimen types is performed. The modelled geometries depict the technical cross-section of the seam, local deviations from the design geometry are not considered. In the investigated numerical evaluations, a partitioning number of four elements at the weld toe for the butt joint and five elements for the T-joint and the longitudinal attachment are applied. The contour plot results are shown in Figure 4. This finite element design is in accordance to the modelling guidelines [13].

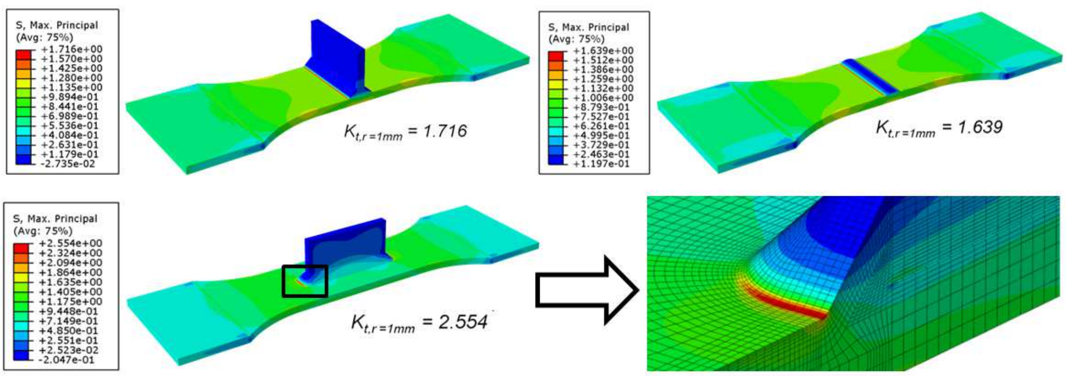

Figure 4: Numerical evaluation of the stress concentration factor K_t

In Figure 5, the computed stress concentration factors for each joint type in dependence of the effective thickness of the ground plate (t_{eff} ranging from *5 up to 25 mm*) and the applied reference radius at the weld toe (r_{ref} ranging from *0.05 up to 2 mm*) are sketched.

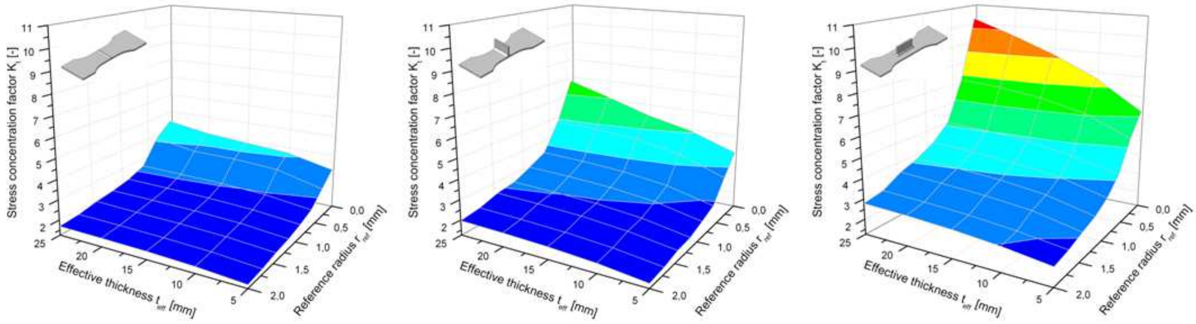

Figure 5: Stress concentration at the weld toe region in dependence of the effective plate thickness t_{eff} and reference radius r_{ref}

After calculation of the notch factors, the thickness (or thinness) correction exponent *n* can be evaluated according to Equation 1. The joint specific results are in agreement to the recommended exponent values for thick joints [1]. A summary of the evaluated non-conservative, thin-walled benefit factors $f(t_{eff}=5\ mm)$ for each specimen type in the as welded and the HFMI treated condition is given in Table 1.

Table 1: Thickness correction exponent *n* and thin-walled benefit factor $f(t_{eff}=5\ mm)$

Specimen type	Condition	n	$f(t_{eff}=5mm)$
Butt joint	As welded	*0.2*	*1.38*
	HFMI treated	*0.1*	*1.17*
T-joint	As welded	*0.3*	*1.62*
	HFMI treated	*0.2*	*1.38*
Longitudinal attachment	As welded	*0.3*	*1.62*
	HFMI treated	*0.2*	*1.38*

3.2 Summary of Fatigue Test Results

To verify the applicability of the benign thinness factor on fatigue, an overview of the nominal stress results is given in Figure 6 to Figure 8. They depict in each subfigure the fatigue behaviour of the base material as well as the, by the non-conservatively thin-walled bonus factor enhanced, structural detail dependent S/N-curve for the untreated (as welded) joint. Finally, the HFMI treated condition is drawn.

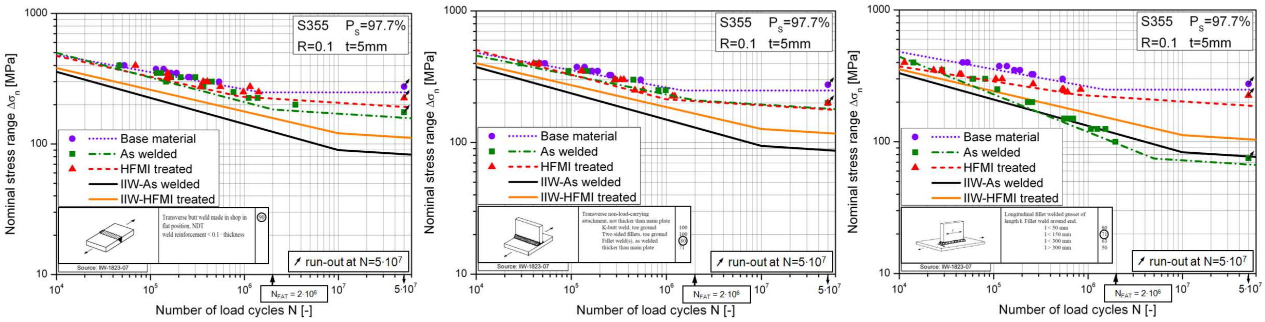

Figure 6: Nominal S/N-curves for *S355*

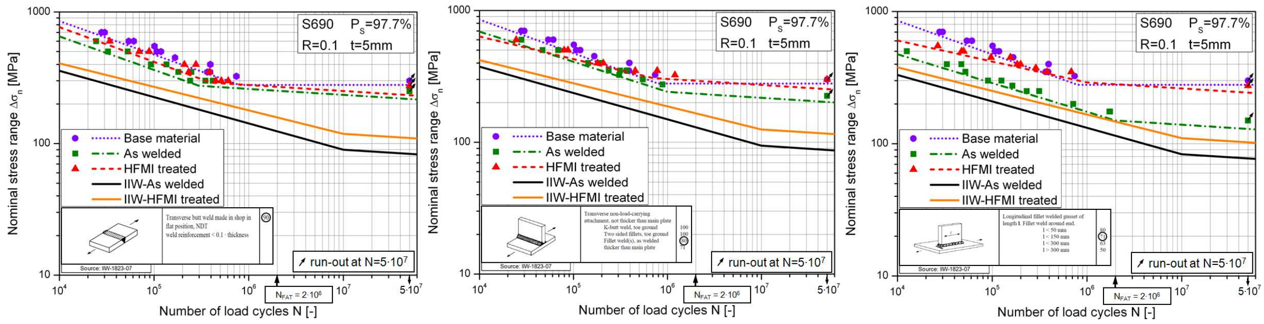

Figure 7: Nominal S/N-curves for *S690*

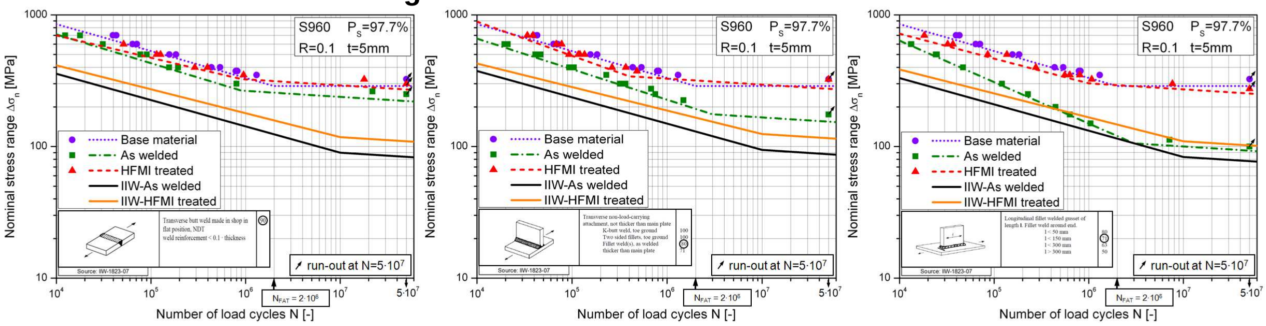

Figure 8: Nominal S/N-curves for *S960*

The fatigue assessment in the finite life regime is performed using the evaluation procedure according to [14] by assuming a log-normal distributed test data. To determine the endurance stress in the high-cycle fatigue region, the arcsin sqrt root transformation is applied to assess the fatigue limit [15]. Both methods use a probability of survival of $P_S=97.7\,\%$ to determine the corresponding FAT-class. As given in the IIW-recommendations [1], a shallower slope of $k=22$ is used for the high-cycle fatigue assessment.
The black solid lines in Figure 6 to Figure 8 mark the structural detail dependent recommended S/N-curves, which are enhanced by the introduced benign thinness factor. It can be seen that the as welded fatigue test points are still above these limits which verify the applicability of the benign thinness factor for the examined joints in the nominal stress approach. For the as welded and HFMI post treated condition, an additional bonus factor of *1.5* is applied. This nominal stress bonus factor is in accordance to the recommendations [1]. Table 2 summaries the endurable stress range at two million load cycles of all examined test series.

Table 2: Endurable stress range at two million load cycles of the investigated test series

Specimen type	**Condition**	**S355**	**S690**	**S960**
Butt joint	As welded	*185*	*250*	*260*
	HFMI treated	*220*	*270*	*315*
T-joint	As welded	*210*	*230*	*195*
	HFMI treated	*210*	*300*	*315*
Longitudinal attachment	As welded	*95*	*150*	*120*
	HFMI treated	*220*	*280*	*295*
Base material	-	*250*	*280*	*290*

A comparison of the nominal stress fatigue test results maintained the following statements:

- For the T- and butt joint, there is only a minor enhancement of the fatigue behaviour due to the HFMI treatment compared to the as welded condition. This is due to the high quality weld process including the use of optimized weld process parameters [6, 7].
- The most significant increase in fatigue is obtained for the longitudinal attachment, which is caused by the small, highly stressed volume at the weld toe at which the local HFMI treatment is very effective.
- In the HFMI treated condition, the common construction steel *S355* reaches for all three specimen types about *85 %* of the base material fatigue stress range and the two high-strength steels *S690* and *S960* are almost equal to the base material fatigue behaviour.
- In the high-cycle fatigue region, the post treatment shows a significant enhancement compared to the finite lifetime regime. An evaluation of the endurable stress range bonus factors *HFMI / IIW-AW* (including benign thinness factor) is shown in Figure 9. The derived bonus factor values depend on the base material yield strength f_y and the stress concentration factor K_t of the investigated specimen types and are evaluated at three different number of load cycles (*N=2e5, 2e6 and 2e7*).

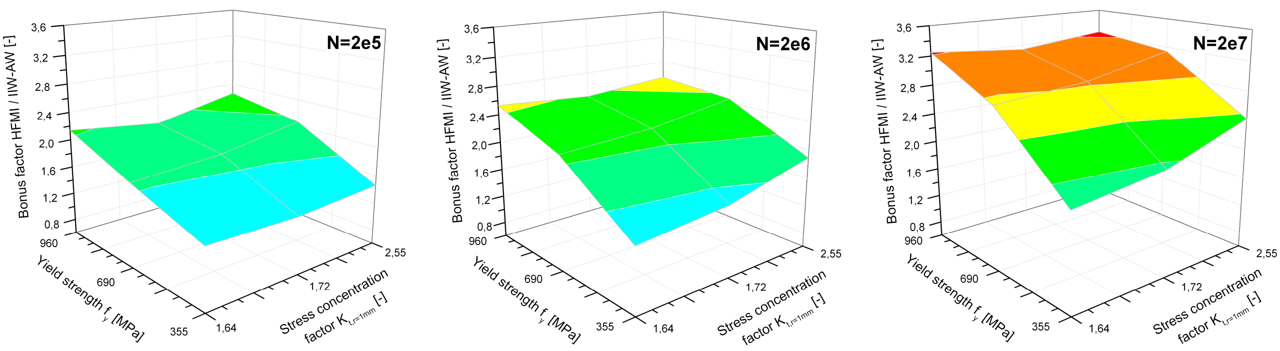

Figure 9: Evaluated nominal endurable stress range bonus factors *HFMI / IIW-AW* at *N=2e5, 2e6* and *2e7* load cycles

- In the nominal stress approach, the HFMI treatment bonus factors seems to be nearly independent of the stress concentration factor K_t due to the achievement of an upmost fatigue behaviour which is close (*S355*) or almost equal (*S690 and S960*).
- The influence of the base material yield strength f_y in dependency of the observed load cycles on the endurable nominal stress range bonus factor *HFMI / IIW-AW* is shown in Figure 10. Thereby, the fatigue strength of the HFMI treated joints increases by applying a higher base material steel grade and rises with a higher number of load-cycles.

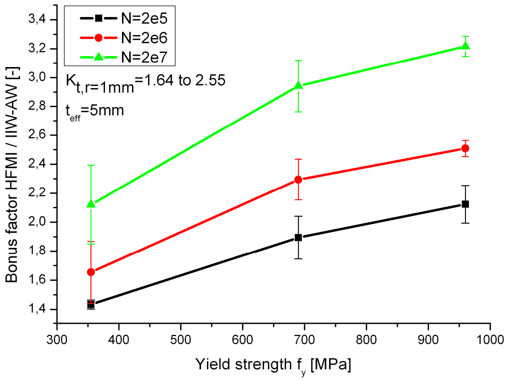

Figure 10: Influence of base material yield strength (nominal stress bonus factor *HFMI / IIW-AW*)

3.3 Strain Gauge Measurements

By measurement of the local strain change, additional information about the stage of technical crack initiation and the subsequent macroscopic crack growth are accessible. Although the number of instrumented specimens is limited, a distinct difference in technical crack occurrence was found between the untreated and the HFMI treated specimens. The applied nominal stress fatigue test range $\Delta\sigma_n$ was between *0.6* and *0.7* of the material strength f_y. A decrease down to *95 %* of the initial measured local strain range was used as assessment criterion. The measured values and the position of the strain gauges at the specimen are shown in Figure 11.

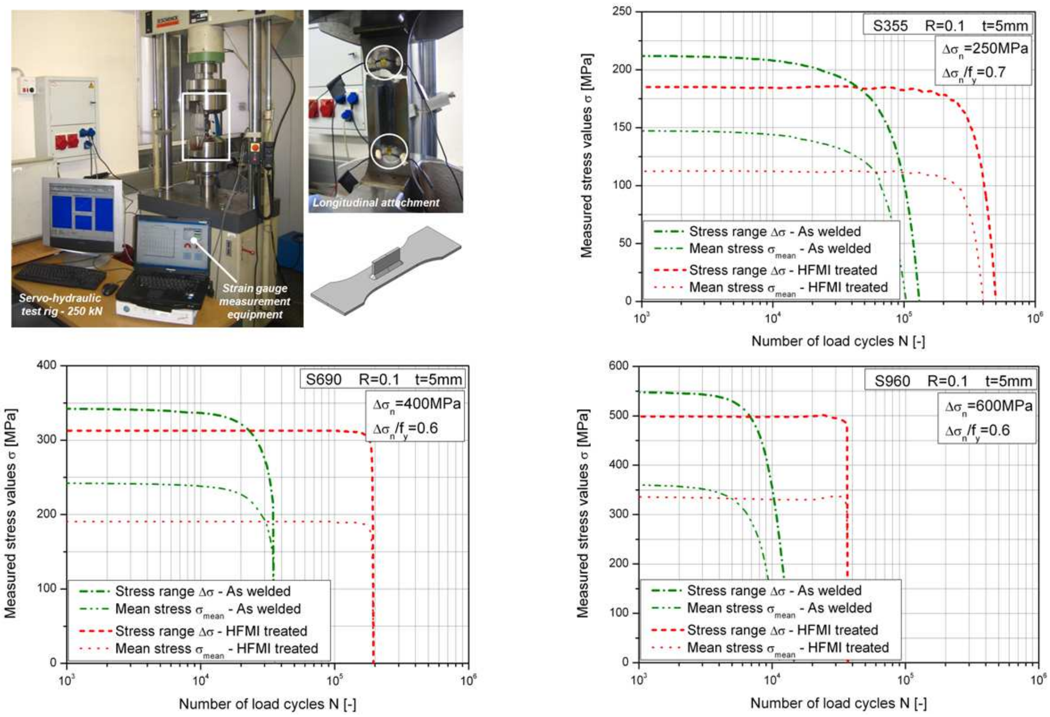

Figure 11: Results of the strain gauge measurements (longitudinal attachment)

The evaluation of the technical crack initiation in Table 3 shows a significant difference between both conditions and the base material yield strength. For the untreated specimens, the technical crack initiates at the common construction steel *S355* at about *10 %* and at the high-strength steels *S690* and *S960* at about *40 %* of the lifetime until rapture N_f. A comparison to the HFMI treated specimens represents higher ratios of about *40 %* for *S355* and *90 %* for *S690* and *S960*. These differences may be caused by crack closure effects due to compressive residual stresses in the weld toe region.

Table 3: Comparison of the technical crack initiation ratio

Crack Initiation	Condition	S355	S690	S960
$N_{\Delta\sigma 95\%}$ / N_f [-]	As welded	*10%*	*40%*	*40%*
	HFMI treated	*40%*	*90%*	*90%*

To improve the measurement of the technical crack initiation, especially for other weld seam geometries as T- and butt joints; it is scheduled to test the applicability of potential driven methods for welded joints made of steel in further investigations.

4. Fatigue Assessment for HFMI treated Joints

4.1 Nominal Stress Approach

In [3], an extensive analysis of published experimental data on the fatigue strength of HFMI treated welded joints shows a procedure to consider the increased fatigue behaviour due to higher base material yield strength in the nominal stress concept. Previous investigations in [16] indicate that a slope of $m=5$ fits the HFMI treated data best. A previous proposal [17, 18] of a design method for HFMI improved joints up to *690 MPa* yield strength defines a strength magnification factor k_y. The factor depends on the strength correction α for yield after HFMI treatment, the reference yield strength $f_{y,0}=355$ *MPa* and the yield strength of the applied base material f_y, see Equation 2.

$$k_y = \alpha \cdot \left(f_y - f_{y,0}\right) / f_{y,0} \tag{2}$$

Based on the procedure given by [3], each fatigue test result (ΔS_i, $N_{F,i}$) can be transformed to two million load cycles using a slope of $m=5$ by Equation 3.

$$\Delta S_i^* = \left((\Delta S_i)^m \cdot N_{f,i} / \left(2 \cdot 10^6\right) \right)^{1/m} \tag{3}$$

For the fatigue assessment, the mean strength $\Delta S_{m,A}$ for each investigated specimen type is used to calculate the yield strength corrected nominal stress range ΔS_i^C, see Equation 4. The evaluation procedure was done in accordance to the statistical methods summarized in [16].

$$\Delta S_i^C = \left(\Delta S_{m,A}\right)^{ky} \cdot \left(\Delta S_i^*\right)^{1-ky} \tag{4}$$

The value of the strength magnification factor can be solved to minimize the standard deviation σ_N of the yield strength corrected nominal fatigue test results. For illustration, the test results without and with yield strength correction for the T-joint samples are pictured in Figure 12. The best fit to this dataset results in a minimized scatter band value of $\sigma_N=0.131$, which is found for a strength correction factor of $\alpha=0.237$.

The mean fatigue strength value for a survival probability of $P_S=50$ *%* at two million load cycles decreases from $\Delta S_m(2e6)=245$ *MPa* down to *205 MPa* due to the strength correction. By minimizing the scatter band, the fatigue strength for a survival probability of $P_S=97.7$ *%* at two million load cycles increases from $\Delta S_k(2e6)=170$ *MPa* up to *180 MPa.*

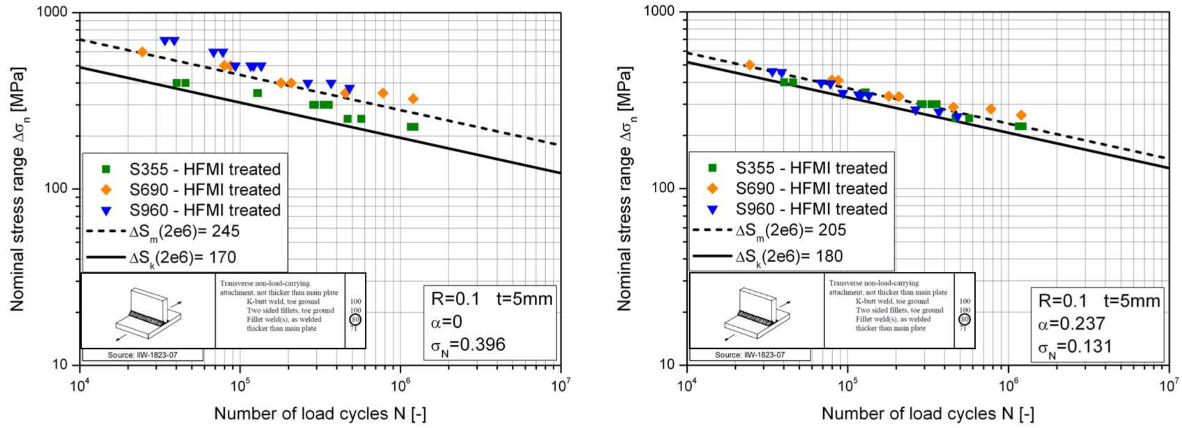

Figure 12: Results for HFMI treated T-joint without (left subfigure) and with f_y correction (right subfigure, α*=0.237*)

To evaluate all three specimen types as a single dataset, the derived fatigue strength values are normalized by dividing both sides of Equation 4 with $\Delta S_{m,A}$, reflecting the individual joint specific structural detail [3].

$$\left(\Delta S_i^C / \Delta S_{m,A}\right) = \left(\Delta S_i^* / \Delta S_{m,A}\right)^{1-ky} \tag{5}$$

Figure 13 depicts the normalized results with f_y correction for all three specimen types. A value of $\alpha=0.277$ leads to a minimum standard deviation of $\sigma_N=0.203$ for the three investigated weld geometries and the three base material combinations. The normalized fatigue strength at two million load cycles lead to a mean value of $\Delta S_m(2e6)=1.75$ and $\Delta S_k(2e6)=1.45$ for $P_S=97.7\,\%$, which is in good accordance to the published results in [3].

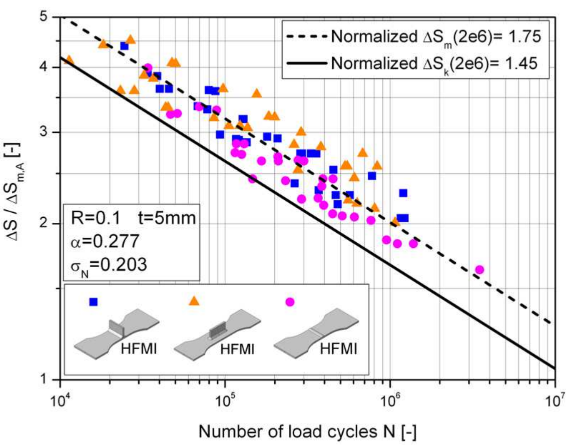

Figure 13: Normalized results for all three specimen types in HFMI treated condition with material strength correction (α*=0.277*)

An overview of the results without ($\alpha=0$) and with ($\alpha>0$) material strength correction, evaluated in accordance to the procedure given in [3], is shown in Table 4. For each specimen type, the mean fatigue strength value ΔS_m decreases due to the correction down to the reference fatigue values of yield strength $f_{y,0}=355\ MPa$. The fatigue strength ΔS_k increases due to the minimized standard deviation σ_N. It has to be noted that in this assessment the slope of the evaluated S/N-curves is fixed to a value of $m=5$ according to [16].

Table 4: Statistical analysis of the investigated specimen types according to [3, 16], see Equations 2-5, with a fixed slope of *m=5*

Specimen type	α	m	ΔS_k [MPa]	ΔS_m [MPa]	σ_N
Butt joint	*0*	*5*	*160*	*239*	*0.437*
	0.289	*5*	*175*	*203*	*0.159*
T-joint	*0*	*5*	*170*	*244*	*0.396*
	0.237	*5*	*180*	*203*	*0.131*
Longitudinal attachment	*0*	*5*	*138*	*223*	*0.518*
	0.283	*5*	*142*	*176*	*0.236*
All joints	*0*	*5*	*1.39 (norm.)*	*2.15 (norm.)*	*0.476*
	0.277	*5*	*1.45 (norm.)*	*1.75 (norm.)*	*0.203*

For comparison purposes, an analysis of the same results without (α=0) and with (α>0) material strength correction by use of a variable slope [14] is performed. The results are shown in Table 5 and reveal a good compliance for the material strength corrected values. In case of no applied strength correction, the slopes of the S/N-curves are decreasing down to a value of approximately *m=3* and therefore also to lower values of ΔS_m and ΔS_k in comparison to Table 4.

Table 5: Statistical analysis of the investigated specimen types, see Equations 2-5, with a variable slope evaluation procedure according to [14]

Specimen type	α	m	ΔS_k [MPa]	ΔS_m [MPa]	σ_N
Butt joint	*0*	*3.4*	*115*	*199*	*0.399*
	0.289	*5.3*	*181*	*207*	*0.158*
T-joint	*0*	*2.9*	*112*	*173*	*0.272*
	0.237	*5.0*	*179*	*203*	*0.133*
Longitudinal attachment	*0*	*2.9*	*73*	*152*	*0.460*
	0.283	*5.4*	*147*	*181*	*0.238*
All joints	*0*	*2.9*	*0.84 (norm.)*	*1.54 (norm).*	*0.381*
	0.277	*4.9*	*1.44 (norm.)*	*1.74 (norm.)*	*0.204*

4.2 Notch Stress Approach

To determine the fatigue strength of HFMI treated joints by the notch stress approach, it is recommended in [13] to model the real weld toe radius by an increased value of one millimetre and evaluate the assessed principal notch stress range against the approvable value of *FAT200.* This procedure is preferable for relatively sharp notches and has not been thoroughly verified.

An alternative procedure for assessing post weld treated joints using the notch stress approach is investigated in [19] and maintains the reference radius of $r_{ref}=1\ mm$ in addition to use a higher FAT-class due to the post weld treatment. Hence, the same stress concentration factors ($r_{ref}=1\ mm$) for the untreated (as welded) and HFMI treated joints are applicable for the assessment. In Figure 14, the local master S/N-curves for the as welded and the HFMI treated condition (base material *S690*) are depicted for further discussion.

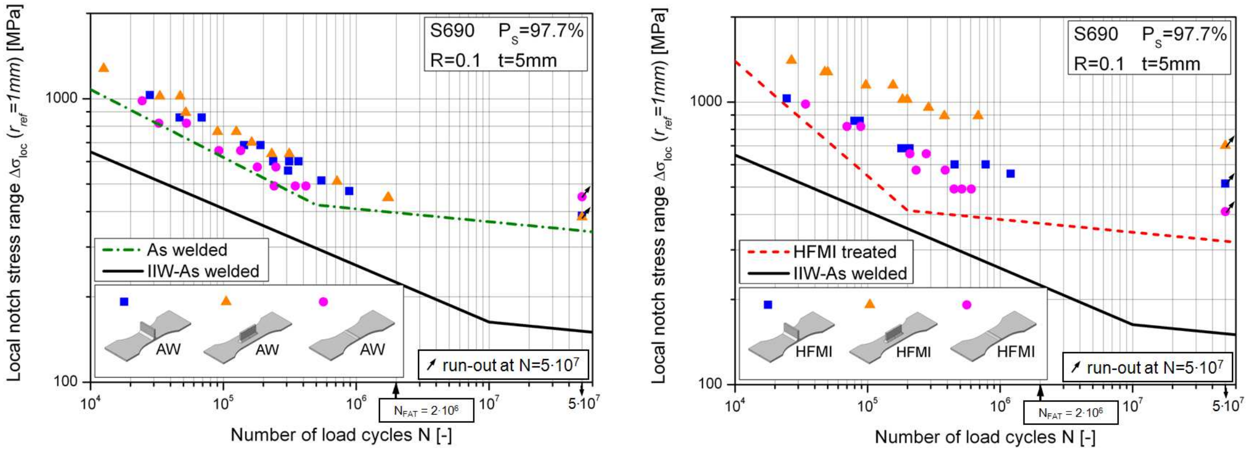

Figure 14: Local master S/N-curves for as welded and HFMI treated condition (*S690*)

In the as welded condition, the investigated specimens show a similar notch stress fatigue range with a relatively small scatter band of $T_S=1:1.28$. The evaluated master S/N-curve is above the recommendation, especially in the high-cycle fatigue region, because of the high manufacturing quality. The local notch stress assessment of the HFMI treated joints shows that the longitudinal attachment is significantly above the other joints due to the high effectiveness of the post treatment for this joint type. The influence of the stress concentration factor K_t is remarkable, which leads to an improper scatter band of $T_S=1:2.30$ by evaluating the master S/N-curve.
The local notch stress approach based on a reference radius of $r_{ref}=1\ mm$ is well applicable in the as welded condition due to the almost identical endurable notch stress range of the investigated specimens. But for the HFMI treated condition, the increase of the fatigue behaviour by the post treatment is different, depending on the local stress concentration at the weld toe, and therefore the obtained master S/N-curve shows an inappropriate high scattering. To improve the assessment of HFMI treated joints by the notch stress concept, an alternative model is introduced as follows.

Figure 15 depicts the principle procedure of the suggested method to assess the local notch stress S/N-curve for HFMI treated joints. The local HFMI notch stress model can be described by three characteristic points:

#1: The base point stress range $\Delta\sigma_B$ at $N_B=2e3$ in the low-cycle fatigue region is influenced by the base material yield strength f_y only:

$$\Delta\sigma_B\left(f_y\right)= p_1 \cdot f_y + p_2 \qquad (6)$$

#2: The current model calculates the slope k_1 in the finite-life fatigue region by using a linear dependency of the yield strength f_y as well as the stress concentration factor K_t, (r_{ref}=1 mm).

$$k_1(K_t, f_y) = K_t \cdot k_{1,gain}(f_y) + k_{1,offset}(f_y) \tag{7}$$

$$k_{1,gain}(f_y) = p_3 \cdot f_y + p_4 \tag{8}$$

$$k_{1,offset}(f_y) = p_5 \cdot f_y + p_6 \tag{9}$$

#3: A fixed transition knee-point of one million load cycles is suggested for simplification. The recommended, shallower slope of k_2=22 is used in the high-cycle fatigue section.

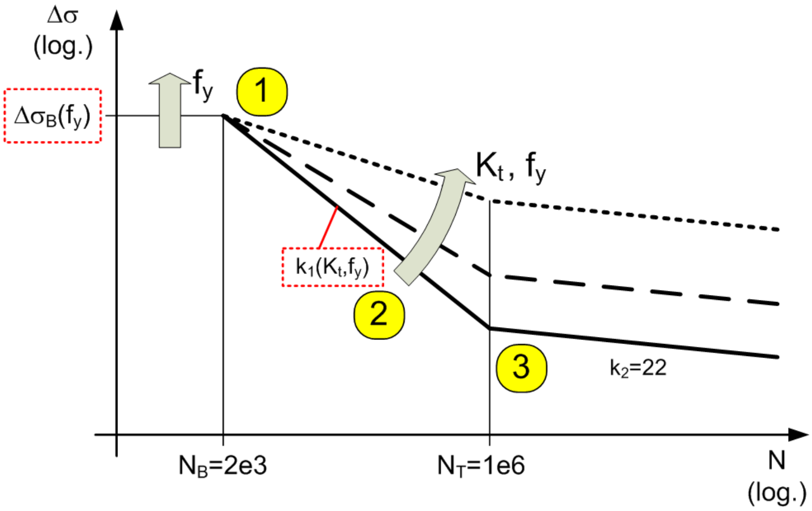

Figure 15: Local master S/N-curve taking the HFMI treatment into account

Current investigations of the thin-walled (t_{eff}=5 mm) steel joints show the basic applicability of a slope-dependent model to assess the increase in fatigue by the HFMI treatment both for different joint types and base material strengths (assuming both a high weld process and HFMI treatment quality).

The application of this HFMI notch stress model is shown in Figure 16. The fatigue test data points are clearly above the evaluated S/N-curves implying a conservative approach. The fixed transition knee point of one million load cycles is a simplification of the current model and can be adopted as material strength dependent value in further work.

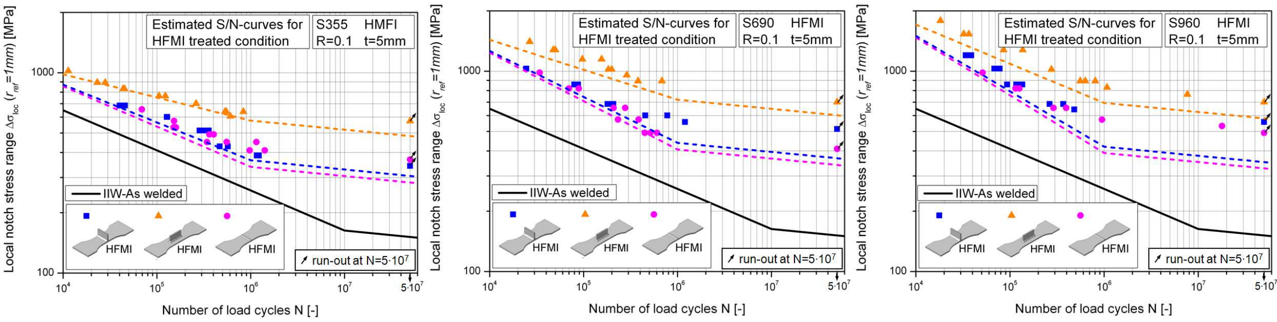

Figure 16: Application of the introduced HFMI notch stress model to experimental fatigue test results

To validate the HFMI notch stress model as a single master S/N-curve, the fatigue test data points are transferred to the shallowest notch stress condition of $K_t=1.6$, which occurs in case of the butt joint. This conversion is done for each test point as ratio of Equation 7 for the investigated joint type, e.g. longitudinal attachment, to the referenced butt joint. The derived data points as HFMI notch stress model with K_t / f_y-slope correction are exemplified in the left subfigure of Figure 17. Finally, the different material classes are unified to *355 MPa* yield strength by the material strength adjustment factor k_y. The observed master S/N-curve in Figure 17, right subfigure, shows a very small scatter band of $\sigma_N=0.138$ which proofs the basic applicability of the introduced model.

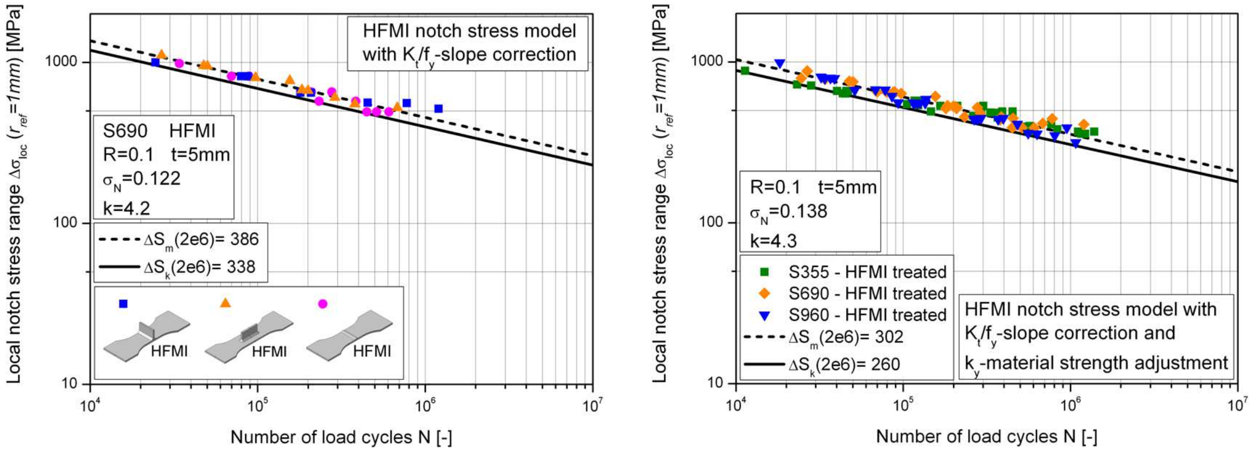

Figure 17: Evaluation of the experimental data points by the HFMI notch stress model as master S/N-curve

The notch stress fatigue behaviour for HFMI treated joints can be basically assessed by the introduced model, but it has to be validated with additional data points further on.

5. Conclusions

Thin-walled longitudinal attachments, T- and butt joints were dynamically tested to determine the influence of the HFMI post-treatment on fatigue. The investigated materials are, a common construction steel *S355,* and two low-alloyed high-strength steels *S690* and *S960*. The plate thickness was overall five millimetres. The weld toe region was HFMI treated without static pre-stressing during the conditioning. The following conclusions have been reached to in this work:

As exemplified in the fatigue test summary section, the base material stress range can be reached for the high-strength steel joints with HFMI treatment. All fatigue test data points are above the IIW-recommendation, even if a bonus factor of *1.5* for HFMI treatment and a benign thinness bonus factor is applied.

The nominal stress assessment of HFMI treated joints was done in accordance to the procedure recently introduced in [3]. The examined test results validated the applicability of the method, leading to a strength correction factor $\alpha=0.277$. All investigated materials and joint types in HFMI treated condition were taken into account to generate this unified nominal S/N-curve.

A novel model to assess the notch stress HFMI fatigue behaviour is introduced. It consists of a material strength dependent base point at two thousand cycles; a material strength and notch stress concentration factor dependent slope in the finite life region; a fixed transition knee point at one million load cycles and a second fixed shallower slope up to the endurance limit. It was shown that this method is applicable to unify the notch stress HFMI fatigue test data into a notch stress master S/N-curve which implies both material and joint type dependency.

Acknowledgements

Financial support by the Austrian Federal Government and the Styrian Provincial Government, represented by Österreichische Forschungsförderungsgesellschaft mbH and Steirische Wirtschaftsförderungsgesellschaft mbH, within the research activities of the K2 Competence Centre on “Integrated Research in Materials, Processing and Product Engineering”, operated by the Materials Center Leoben Forschung GmbH under the frame of the Austrian COMET Competence Centre Programme, is gratefully acknowledged.

Special thanks are given to the Austrian Research Promotion Agency (FFG), who founded the research project by funds of the Federal Ministry for Transport, Innovation and Technology (bmvit) and the Federal Ministry of Economics and Labour (BMWA), and to all the industry partners for the supply of material and the fabrication work done.

References

[1] Hobbacher A.: IIW Recommendations for Fatigue Design of Welded Joints and Components, WRC Bulletin 520, The Welding Research Council, New York, 2009.

[2] Haagensen P.J. and Maddox S.J.: IIW Recommendations on Post Weld Improvement of Steel and Aluminum Structures, IIW-Doc. XIII-2200r3-07, revised 2009.

[3] Yildirim H.C. and Marquis G.B.: Fatigue strength improvement factors for high strength steel welded joints treated by high frequency mechanical impact, Intern. Journal of Fatigue, 2012.

[4] Marquis G.B.: Failure modes and fatigue strength of improved HSS welds, Engineering Fracture Mechanics, Vol. 77, pp. 2051-2062, 2010.

[5] Leitner M. and Stoschka M.: Influence of steel grade on the fatigue strength enhancement by high frequency peening technology on longitudinal fillet weld gusset, Journal of Engineering and Technology, vol. 1, issue 3, pp. 80-90, 2012.

[6] Stoschka M., Leitner M., Fössl T. and Posch G.: Effect of high-strength filler metals on fatigue, Welding in the World, vol. 56, no. 3/4, pp. 20-29, 2012.

[7] Stoschka M., Leitner M., Posch G. and Eichlseder W.: Effect of high-strength filler metals on the fatigue behaviour of butt joints, Welding in the World, vol. 57, no. 1/2, 2013.

[8] Barsoum Z.: Fatigue design of welded structures – some aspects of weld quality and residual stresses, Welding in the World, vol. 55, no. 11/12, 2011.

[9] Pitec GmbH, http://www.pitec-gmbh.com/.

[10] Statnikov E.S., Muktepavel V.O. and Blomqvist A.: Comparison of Ultrasonic Impact Treatment (UIT) and Other Fatigue Life Improvement Methods, Welding in the World, vol. 46, pp. 28- 39, 2002.

[11] Sonsino C.M.: Effect of residual stresses on the fatigue behaviour of welded joints depending on loading conditions and weld geometry, Intern. Journal of Fatigue, Vol. 31, pp. 88-101, 2009.

[12] Leitner M., Stoschka M., Schörghuber M. and Eichlseder W.: Fatigue behaviour of high-strength steels using an optimized welding process and high frequency peening technology, Proceedings of the Intern. Conference of the IIW, pp. 729-736, 2011.

[13] Fricke W.: Guideline for fatigue assessment by notch stress analysis for welded structures, IIW-Document XIII-2240r1-08 / XV-1289r1-08, 2008.

[14] ASTM International: Standard Practice for Statistical Analysis of Linear or Linearized Stress-Life (S-N) and Strain-Life (ε-N) Fatigue Data, Designation: E739-91, reapproved 1998.

[15] Dengel D. and Harig H.: Estimation of the fatigue limit by progressively-increasing load tests, Fatigue & Fracture Engineering Materials & Structures, vol. 3, issue 2, pp. 113-128, 1980.

[16] Yildirim H.C. and Marquis G.B.: Overview of Fatigue data for high frequency mechanical impact treated welded joints, Welding in the World, vol. 57, no. 7/8, 2012 (in print).

[17] Weich I.: High frequency hammer peening design, Presentation to IIW-Commission XIII WG2, 2009.

[18] Weich I. Fatigue behaviour of mechanical post weld treated welds depending on the edge layer condition (Ermüdungsverhalten mechanisch nachbehandelter Schweißverbindungen in Abhängigkeit des Randschichtzustands). Technischen Universität Carolo-Wilhelmina, Doctorate Thesis, 2008.

[19] Pedersen M.M., Mouritsen O.Ø., Hansen M.R. and Andersen J.G.: Experience with the Notch Stress Approach for Fatigue Assessment of Welded Joints, Swedish Conference on Light Weight Optimized Welded Structures, pp. 122-133, 2010.